Influence of IMU's Measurement Noise on the Accuracy of Stride-Length Estimation for Gait Analysis

Guillermo García-Villamil[1], Luisa Ruiz[2], Antonio R. Jiménez[3], Fernando Seco[4] and M.C. Rodríguez-Sánchez[5]

,2,3,4[1] *Centro de Automática y Robótica (CAR). CSIC-UPM. Ctra. Campo Real km 0.2, 28500 Arganda del Rey, Spain.*
[5]*URJC, 28933 Móstoles (Madrid), Spain.*

Abstract
Inertial Measurement Units (IMUs) are used to analyse human gait in health monitoring applications. Parameters such as step or stride length, speed, cadence or balance/support times, are important to determine degenerative states in people, e.g. frailty. The estimation with accuracy and precision of significant gait parameters is important to reliably discriminate between groups of patients, e.g. separating groups affected by pathologies from those without problems. In this work, we analyze how the noise content in a IMU (Bias stability and Random walk), measured by Allan variance analysis, as well as, the selected measurement range in accelerometers and gyroscopes, can influence the stride length (SL) estimation, which is one of the most discriminant gait parameters in the literature. IMUs from different manufacturers have been characterized for noise performance, and then compared for accuracy in stride length estimation, by mounting them in the feet of several subjects in gait analysis tests. For this purpose, we used an inertial integration method with zero velocity updates at stance detection (INS-ZUPT), checking its accuracy against a set of ground marks of known length as a true reference. Our results show that stride-length estimation algorithms are relatively tolerant of the IMU's measurement noise and range; however, step detection algorithm performance, ZUPT corrections, quality of IMU calibrations and the secure IMU attachment on the foot to avoid oscillations, are all important issues for accurate Stride-Length estimation.

Keywords
IMU, gait, noise, sensing range

1. Introduction

According to the World Health Organization, in the next decades the proportion of the world's population over the age of 60 will double from 11% to 22% [1]. A major challenge for health care systems worldwide is the accompanying increase in geriatric diseases, involving high costs and a large social impact. One of the most prevalent is frailty, which is a a clinically state of

IPIN 2021 WiP Proceedings, November 29 – December 2, 2021, Lloret de Mar, Spain
guillermo.gv@csic.es (G. García-Villamil); luisa.ruiz@csic.es (L. Ruiz); antonio.jimenez@csic.es (A. R. Jiménez); fernando.seco@csic.es (F. Seco); cristina.rodriguez.sanchez@urjc.es (M.C. Rodríguez-Sánchez)
https://lopsi.car.upm-csic.es (A. R. Jiménez); https://lopsi.car.upm-csic.es (F. Seco); https://sites.google.com/view/senialab-mostoles/ (M.C. Rodríguez-Sánchez)
0000-0002-3869-4410 (G. García-Villamil); 0000-0003-0316-7781 (L. Ruiz); 0000-0001-9771-1930 (A. R. Jiménez); 0000-0002-2922-2710 (F. Seco); 0000-0001-9243-2166 (M.C. Rodríguez-Sánchez)

increased vulnerability caused aging-associated decline of physiologic system, and it is related with the increases in mortality, fall risk and hospitalization [2].

Gait analysis is one of the most commonly used methods to detect frailty and fall risk in elderly people [3]. The development of technological systems has improved the possibility for accurate and objective gait analysis, leading to better diagnosis and treatment of associated degenerative diseases. Several studies have considered the use of sensors to analyze the differences between groups of patients (with or without problems) from some spatio-temporal parameters like stride length (SL), speed, stance time or swing time [4]. Stride length is considered a significant parameter in many reviews [5, 6] [7], in which SL is defined as a parameter to diagnose frailty, related with fall risk and able to discriminate between patients groups.

Numerous traditional technologies are available in gait analysis: pressure walkways, optical systems, force platforms and foot switches. However, recently the use of inertial measurement units (IMUs) has increased due to their advantages: low cost, accuracy, size and portability [8]. IMUs measure angular velocity and linear acceleration making use of the built-in 3-axes gyroscopes and accelerometers, respectively. From that data the different phases in a walking cycle are detected in order to estimate the gait parameters. One of the main methods used in the literature (and also in this work) is foot-mounted inertial integration with zero velocity updates at stance detection (INS-ZUPT) [9]. This algorithm consists on first detecting step events using patterns in accelerations or gyroscopic signals, and then integrating acceleration to obtain velocity with drift corrections (zero velocity updates) every time a step is detected. This approach assumes that velocity is zero when the foot is in the stance phase, so it resets accumulated velocity errors and improves the velocity estimate during swing phase (needed to obtain an accurate stride length estimation).

To achieve a right discrimination between patient groups, it is necessary to obtain the gait parameters as accurately and precisely as possible. Noise from sensors (gyroscopes and accelerometers) and the signal acquisition conditions and operating range can affect the correct estimation of gait parameters.

For example, some studies [10], have questioned the hypothesis of whether the sensor's velocity is exactly zero during the stance phase and quantified the stride length estimation error for different gait speeds. Even, when the foot is flat on the terrain, depending on the IMU mounting position (heel, insole, etc.) some rotations and displacements can be registered on the IMU, affecting estimations[11].

Other works study the performance of stride length estimation methods, by comparing them to an external reference such as 3D motion analysis systems or a walkway with pressure sensors. In [12] we find a comparison of IMU-foot mounted INS-ZUPT algorithms under different attitude estimation methods (rotation matrix and quaternions). For some tests made in walking distances of 3.5 m and 3 different velocities, this work shows stride length errors smaller than 5-6%, which is sufficient for the discrimination between healthy and pathological subjects.

The influence of the noise in ZUPT estimation are analysed in [13]. However, this study used a single IMU with a simulation model. In [14] the effect of the accelerometer operating range (OR) on stride length estimation is analyzed, but for running activities. Their findings of using accelerometers with a minimum OR of 32 g (gravitational force unit) to obtain accurate measurements is not applicable for our goal (frailty monitoring). We can operate with acceleration ranges between 8 and 16 g maximun. In [15] they evaluate the gait analysis algorithm proposed by [16] with tests using different step lengths. Results shows a SL RMSE equal to 3% compared with a gold standard (or ground-truth) OptoGait. However they do not test the effect of speed variation on SL estimation.

Recalling the works described above, the aim of this study is to analyze how the noise and the operating range influence the value of the gait parameters, SL in particular, using different commercial IMUs and multiple stride lengths and speeds. The IMUs will be attached to the foot and an INS-ZUPT algorithm will be used.

We will use the following methodology: First, we will quantify the error of 3 different IMU by Allan variance analysis (AVA) with different operating ranges. Next, we perform tests with the 3 IMUs mounted on the right-foot of five persons, walking at two different speeds and two "forced" stride lengths (0.8 m and 1.6 m). Raw IMU signals are processed using a step detection and INS-ZUPT algorithm to obtain the SL. Finally, an SL error evaluation is performed using a reference that consists of marks on the ground of known lengths.

The paper is organized as follows: section 2 gives a description of the noise analysis of each IMU, while section 3 describes the experiments, tests and algorithms carried out. Results and discussions are presented in section 4. Finally section 5, provides some conclusions and outlines future work.

2. Noise Analysis of IMUs

Inertial motion units contain microelectromechanical systems (MEMS) such as accelerometers and gyroscopes, which can be used for the estimation of gait parameters, such as steps counts, stride lengths (SL), velocity, and other variables by integrating the output data of the IMU. Modern IMUs contain a microprocessor with relatively complex inertial navigation system (INS) algorithms which process the raw sensor data.

While very convenient for their size and cost, MEMS sensors are far from ideal, suffering from deterministic and stochastic errors. The deterministic errors, such as misalignment, different axes gains or biases are almost constant through time, and therefore can be eliminated by proper calibration. On the other hand the stochastic errors follow a given error distribution model but are unpredictable and can not be factory-calibrated. Even after calibration, the remaining stochastic noise is accumulated during the IMU raw-data integration in the INS stage, causing orientation and velocity estimations which drift exponentially with time, making spatial or gait estimations (e.g. SL) to be less accurate.

2.1. Allan Variance Analysis

For the analysis of stochastic errors a commonly used method is *Allan Variance Analysis* (AVA) [17], which represents the root mean square (RMS) random error of the IMU output data as a function of an averaging interval. Previous works explain this method [18, 19] in detail, but here we shortly introduce its fundamentals and how to use it.

The Allan Variance of a N-long sampled data sequence $S = \{S_k | k = 1..N\}$, of accelerations or angular rates, can be computed from the difference between the averages of consecutive data bins of size m each, as [20]:

$$\sigma^2(\tau) = \frac{1}{2(n-1)} \sum_{i=1}^{n-1} \left(\overline{S}_{k+m} - \overline{S}_k\right)^2 \tag{1}$$

where τ is the time duration of a data bin of size m around the k sample, $\overline{S}_k$ is the average sensor's value of that data bin with m samples (computed as $m = \tau/\Delta t$, being Δt the sampling time); and n is the resulting number of bins in the sequence ($n = N/m$).

If we integrate the data sequence S, into a variable $\theta = \{\theta_k | \theta_k = \sum_{i=1}^{k} S_i\}$, then the Allan Variance can alternatively be computed as [17]:

$$\sigma^2(\tau) = \frac{1}{2\tau^2(N-2m)} \sum_{k=1}^{N-2m} \left(\theta_{k+2m} - 2\theta_{k+m} + \theta_k\right)^2 \tag{2}$$

The Allan Variance method assumes that the noise present in the sequence is the additive combination of several random processes that have separable behaviors in a plot of the Root Allan Variance $\sigma(\tau)$ vs. τ on a logarithmic-logarithmic scale. To estimate the ARW or VRW (Angular/Velocity Random Walk, for Gyros and Accelerometers respectively), it is required to read the value of $\sigma(\tau)$ with slope $-\frac{1}{2}$ at $\tau = 1$. The Bias Instability or BRW can be determined studying the flat region of the Root Allan Variance; the BRW value is found as $\sigma(\tau)_{\text{slope}=0}/0.664$. Other noise models parameters can be derived (quantization, sinusoidal, Rate-Random-Walk RRW [13]) but the ARW (white noise) and the BRW (bias instability) are the main random parameters used to model noise in most MEMS IMU sensors. If these parameters are high, this means that the noise in the IMU is high, which might affect the estimations of gait parameters.

In this study, we analysed the Angle/Velocity Random Walk (ARW/VRW) and Bias Instability (BRW) for several IMUs available at our laboratory.

2.2. AVA experimentation with 3 different IMUs

We conducted several static long-term recording tests (24 hours), on a cushioning surface, in order to obtain data for the AVA analysis of each IMU. We repeated tests using different measuring ranges for both accelerometers and gyroscopes. The IMUs selected for this study are:

- LSM6DS3 from STMicroelectronics. The IMU has a triple-axis orthogonally oriented accelerometer and gyroscope. The IMU can be adjusted with different ranges, $\pm 2/4/8/16$ g for the accelerometer and $\pm 125/250/500/1000/2000$ dps (degrees-per-second) for the gyroscope. Sampling frequency was set to 104 Hz. No explicit calibration was done. This sensor belongs to an integrated Arduino Nano 33 IoT board with a microSD socket (where log files were stored) and wireless connectivity. The device used corresponds to the final degree work of one of the authors [21]. The dimensions of the device are 78x45x38 mm, its weight 79 g and its components cost is about 100 (excluding labor).
- Osmium MIMU22BL from Inertial Elements. This inertial device is an array of 4 IMUs whose outputs are fused together to provide a virtual unique IMU with the usual tri-axes accelerometers, gyroscopes and magnetometers. The model allows Bluetooth v4.1 and

USB 2.0 communications. Accelerometers and gyroscopes can be adjusted to operate with different ranges such as: $\pm 2/4/8/16$ g and $\pm 125/250/500/1000/2000$ dps. Sampling frequency was set to 62.5 Hz. Data was collected, using a BLE connection, with a personal computer (PC) running a Matlab 2019b script (class MIMU22BL). Sensor dimensions are 31.0 x 23.5 x 13.5 mm, weight is 12 g and price is 400 .

- Xsens MTi. The IMU has a triple-axis orthogonally oriented accelerometer, gyroscope and magnetometer. The IMU range is $\pm 50\ m/s^2$ and ± 300 dps. Sampling frequency is adjusted at 100 Hz. Dimensions: 58x58x22 mm, weight: 50g and price: 2.360 . This sensor from Xsens was purchased in 2007, so it has a lower performance compared to new versions currently available at Xsens (MTi 100-series). For this unit, data was collected by USB connected to a PC running the the Xsens sensor manager. The recorded binary log file was parsed with a Matlab script using the licence keys and MotionTracker COM object libraries on a 32-bit Matlab 2017 version.

For the accelerometers, in the AVA of Figure 1 and Table 1 we can observe that XSENS outperforms MIMU22BL and LSM6DS3, being LSM6DS3 the worst. Only in LSM6DS3 we can appreciate a slight improvement in the accelerometer noise when the range is lowered. However, in the gyroscope AVA analysis in Figure 2 and Table 2 we can observe that MIMU22BL outperforms LSM6DS3 and XSENS, being XSENS the worst.

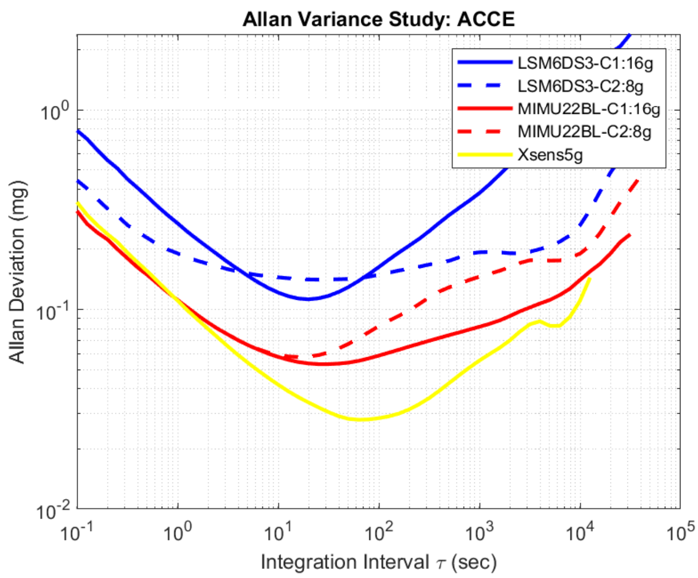

Figure 1: Allan Variance Study of accelerometer noise.

The found diversity in the IMU noise performance analysis results interesting so as to see how these different features propagate to the SL estimation accuracy. Next section explores several walking experiments with different subjects and walking styles to study the SL estimation performance.

Table 1
Allan Acc

IMU model	Range	VRW $(m/s)/\sqrt{h}$	BWR mg
LSM6DS3	16 g 8 g	0.14 0.07	0.17 0.21
MIMU22BL	16 g 8 g	0.07 0.07	0.08 0.09
Xsens	5 g	0.06	0.04

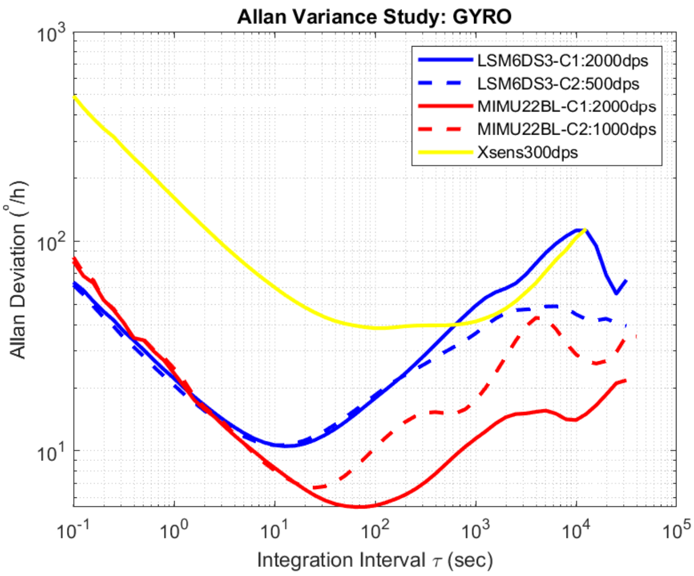

Figure 2: Allan Variance Study of gyroscope noise.

3. IMU Calibration

Calibration is carried out so as to correct the deterministic errors such as misalignment, different axes gains or biases, which are almost constant through time, although dependent on temperature.

This calibration sometimes is carried out by the producer, with high tech and sophisticated equipment's (e.g. precise rotation tables and temperature controlled chambers), which are really expensive. Xsens delivers all their products with this high quality calibration. MIMU22BL is also factory calibrated but without this equipment. LSM6DS3 is not factory calibrated.

Analysing the different methodologies proposed for IMU calibration without equipment's, we decided to conduct the one proposed by Teldadi [22], which relies on orienting the IMUs to different poses, and then performing an optimization of a cost function using a Marquant-Levenbenverg (ML) non-linear minimization algorithm. The method provides calibration in both

Table 2
Allan GYR

IMU model	Range	ARW $^\circ/\sqrt{h}$	BRW $^\circ/h$
LSM6DS3	2000 dps	0.41	15.84
	500 dps	0.38	16,02
MIMU22BL	2000 dps	0.40	8.13
	1000 dps	0.45	10.04
Xsens	300 dps	2.66	57,96

accelerometers and gyroscopes for misalignment, axes gains or biases. This method was selected, apart from being cost-effective and they provide enough implementation details, because they made exhaustive validation tests with simulated noise and also by comparing calibration results with those certified for a particular Xsens-MTi calibration chart.

In addition to misalignment and axes gains, we also observed significant delays in the time stamps of MIMU22BL and LSM6DS3, so we proposed to conduct a simultaneous clock calibration, in this way extending the work of Teldadi [22]. This poor clock performance observed in MIMU22BL and LSM6DS3 is due to the internal components of each sensor, LSM6DS3 uses an internal oscillator as the clock source for the microcontroler, which is very inaccurate. The detected poor clock performance (about 1% deviations from true time) affects in the stride length estimation through the double integration of IMU data, first affecting orientation, and then affecting to the the gravity that leaks into the velocity and space estimations.

The calibration requires to obtain raw IMU data in diverse poses. Firstly the IMU must be placed static for 50 seconds, then it must be rotated in different orientations every 4-5 seconds, with at least 22 orientations (recommended 38 to 60 different positions). Multiple positions are required to create a system of equations with 9 unknowns for accelerometers, 12 unknowns for gyroscope, and one for time. For this purpose, we have fabricated, with a 3D printer, a 60 faced polyhedron shown in figure 3, called pentakisdodecahedron, for the IMU calibration process where IMUs are placed inside of this polyhedron.

Figure 3: 3D printed pentakisdodecahedron used for the calibration of the different IMUs.

The algorithmic calibration process, sketched in Figure 4, consists of the following steps:

1. *Accelerometer Calibration.* The 3-axes accelerometer is calibrated by comparing the gravity magnitude in each static position with the accelerometer data, and performing a ML minimization.
2. *Clock Calibration.* To calibrate the clock data, first we use the calibrated accelerometer data, and remove the gyroscope bias ("Gyr Unbiased" in Figure 4) obtained from still poses. Then Gyroscope data is integrated through the rotation process between statics positions, and comparing this integrated rotation with the position offered by the gravity vector in the static position, another ML minimization is executed to obtain the clock delay. This difference in the estimation of the orientation, by integrating gyroscope data through time, with the gravity vector allow us to estimate the error in the sample rate of each IMU.
3. *Gyroscope Calibration.* Finally, we calibrate the gyroscope alignment and scale, using the previously calibrated accelerometer and clock. This process uses the same cost function as in the Clock Calibration, but considering sampling time as a known element.

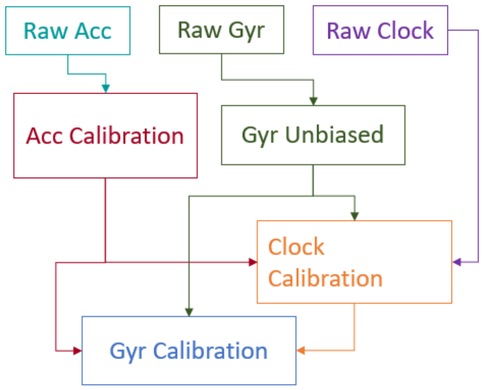

Figure 4: Algorithmic calibration process with three consecutive stages: 1) "Acc Calibration", 2) "Clock Calibration", and 3) "Gyr Calibration".

Using the above described methods, we conducted this calibration process for LSM6DS3 which is not pre-calibrated and for MIMU22BL which has not a solid pre-calibration process. The results of calibration process for MIMU22BL and LSM6DS3 are in Tables 3, 4 respectively.

4. Walking experimentation and method for stride length estimation

We show next the tests and algorithms for SL estimation.

4.1. IMU attachments, subjects and walking conditions

A total of 5 subjects with age 36±13 and height 176±10, were equipped with 3 IMUs attached to each of them on the right foot's instep, as shown in Figure 5.

Table 3
MIMU22BL calibration parameters

Acc misaligment			Acc scaling			Acc bias
1	0.0005	-0.0045	0.9994	0	0	-0.0951
0	1	-0.0011	0	0.9993	0	0.0943
0	0	1	0	0	0.9951	-0.0696
Gyr misaligment			**Gyr scaling**			**Gyr bias**
1	0.0024	-0.0052	0.9992	0	0	-0.0072
-0.0077	1	0.0062	0	1.0041	0	-0.0109
0.0046	0.0034	1	0	0	0.9905	-0.0001
Time Calibration factor:			1.0102			

Table 4
LSM6DS3 calibration parameters

Acc misaligment			Acc scaling			Acc bias
1	-0.0004	-0.0005	0.0048	0	0	28.053
0	1	-0.0027	0	0.0048	0	10.441
0	0	1	0	0	0.0048	4.621
Gyr misaligment			**Gyr scaling**			**Gyr bias**
1	0.0052	-0.0097	0.0012	0	0	21
0.0029	1	-0.0134	0	0.0012	0	-29
-0.0066	-0.0077	1	0	0	0.0012	-55
Time Calibration factor:			0.9912			

Sensing range was adjusted to 16 g and 2000 dps for all IMUs, while the sampling frequency was 100 Hz for XSENS, 104 Hz for LSM6DS3 and 62.5 Hz for MIMU22BL. The IMUs could not being adjusted at the same frequency so we chosen the closest values to 100Hz with reliable transmission.

Four types of tests have been carried out. Each of them consist of walking 8 m in straight line, on a tiled floor. The edge of each tile is used as a marker, to take steps of known length. Two different strides lengths, 0.8 m and 1.6 m, and two velocities, slow and fast have been used. So, the 4 walking modes are:

- *Test 1*: 6 steps of SL equal to 0.8 m and slow speed.
- *Test 2*: 3 steps of SL equal to 1.6 m and slow speed.
- *Test 3*: 6 steps of SL equal to 0.8 m and fast speed.
- *Test 4*: 3 steps of SL equal to 1.6 m and fast speed.

Each test has been carried out 2 times by 3 different subjects, for a total of 200 recorded log files and 1500 steps. Afterwards, slow and fast gait velocities were calculated with an average value of 0.4 and 0.8 m/s, respectively.

Figure 5: Attachment of the IMUs on the right foot of one test subject.

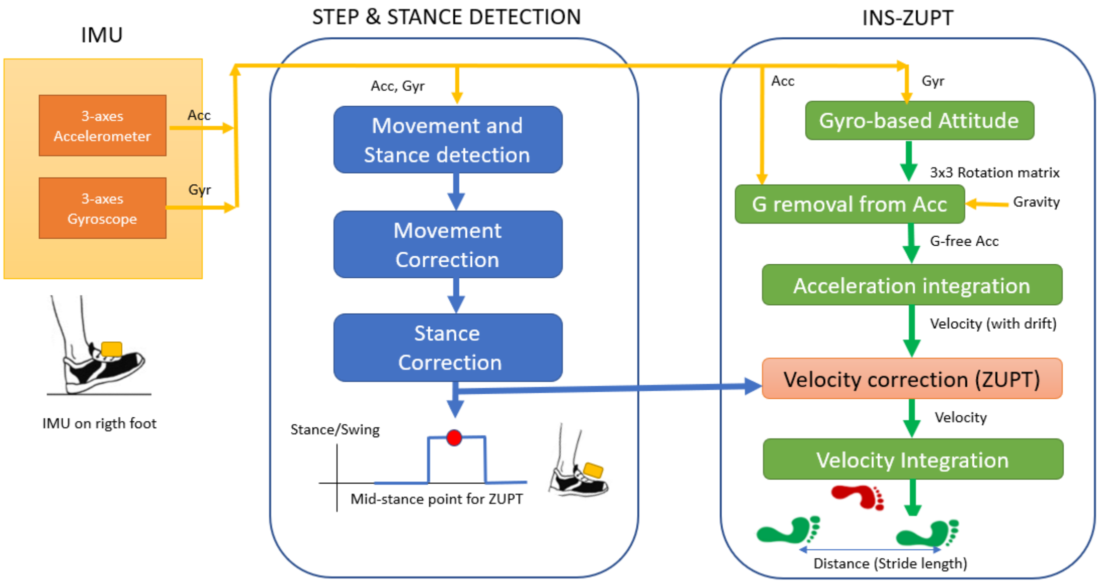

Figure 6: Stride length estimation algorithm using a multi corrector stance detection and Zero Velocity Update (ZUPT)

4.2. Data processing for SL estimation (Multi corrector INS-ZUPT)

Data collected was processed using a Pitch-based INS-ZUPT algorithm implemented in Matlab (see Fig. 6). It analyses the pitch angle's of the foot distinguishing the swing phase from the stance phase (walking phase where the foot is momentarily resting on the ground). Stance phase is used to reset velocity to zero, and during swing phase the SL is computed using an INS algorithm.

The stance detection algorithm consists of the next steps:

1. *Movement and Stance detection.* In order to reduce the miss detection of some steps, we apply loose thresholds for accelerometer and gyroscope data, resulting in over movement and stance detection. Firstly, when accelerometer and gyroscope data are under the low

threshold ($Th1 = 1m/s^2$ or π/s) stance detection phase is detected. Secondly, when accelerometer and gyroscope data are above the upper threshold ($Th2 = \sqrt(2)m/s^2$ or π/s) movement detection phase is detected. Moreover, these thresholds were constant through every single test.

2. *Movement Correction* . To reduce the over movement detection we apply the following conditions.
   a) Eliminate close movement detected periods.
   b) Eliminate short movement detected periods.
3. *Stance Correction* . To reduce the over stance detection we apply the following conditions.
   a) Eliminate stance detected periods without a previous detected movement period, in a short window.
   b) Reduce large stance detected periods, to the average stance period distance.
   c) Eliminate short stance detected periods.

Figure 7 shows the step detection result process

The step detection (SD) process is not straightforward. Many works report frequent SD failures even in regular walking conditions. We used this multi corrector method instead the one proposed in [9] because it could not be adjusted to our challenging testing conditions (very different step lengths, speeds and the intrinsic difference between gait individuals), we also try to implement the Jerkage method proposed in [23], however we did find impossible not to adjust in each trial the threshold required for this method for acceptable results. Figure 7 shows the step detection result process: black lines represent the accelerator and gyroscope values, blue and magenta lines represent the high and low pitch, the red squared line is stance, and each detected step is plotted by a red point.

Once stances are found, INS-ZUPT algorithm [9] is applied. It consists in the following stages:

1. *Remove gravity.* Sensor signals are transformed from the sensor (S) to the global (G) navigation frames using a rotation matrix estimated with the gyroscopes. Since the Z-axis is vertical, the gravity can be removed from the accelerometer signals ($Acc_zG = Acc_zG -$ gravity).
2. *Integrate g-free acceleration.* Integration of the acceleration provides the linear velocity: Vel_G; however, this estimate suffers from strong drift.
3. *Apply ZUPT.* Eliminate the drift in the linear velocity estimate by using the ZUPT update at every stance event, since we know that at this instant the foot is static. Velocity correction can be seen in Figure 8: when a step is detected (red point), velocity values are set to zero.
4. *Velocity integration for SL.* Corrected velocity is integrated to obtain linear displacement and positions. The stride length, SL is the position difference between two consecutive steps.

5. Result & Discussion

This section describes the results from the tests and algorithms above explained, including the mean SL values for each test and IMU, the standard deviation and total distance errors.

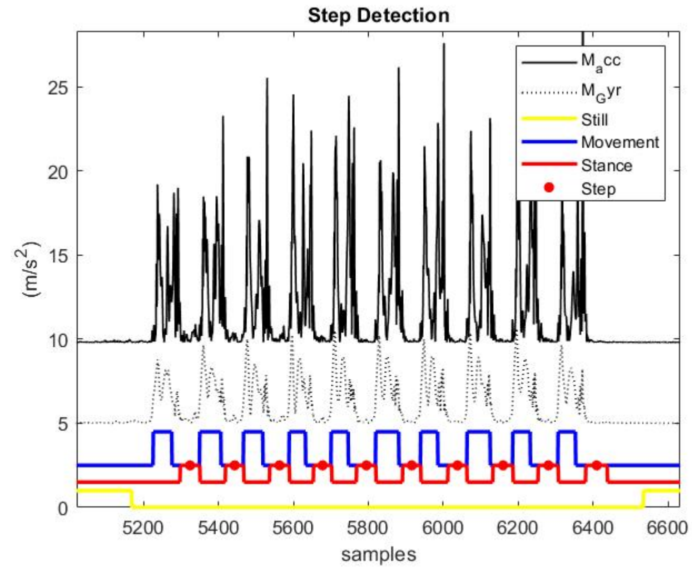

Figure 7: Results of the step and stance detection algorithm. Black lines are the accelerations and gyroscope outputs, blue line the movement, red line corresponds to stance and red points to detected steps.

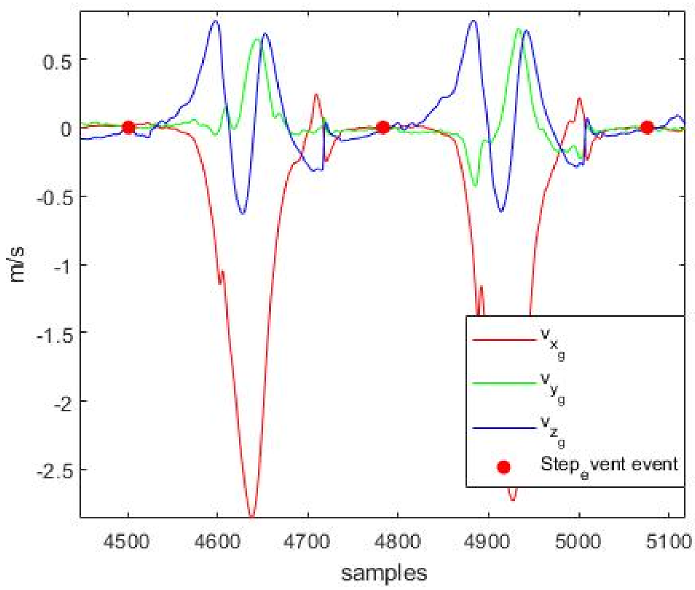

Figure 8: Integrated linear velocities with the ZUPT method. The red, green and blue lines correspond to x,y,z- components of velocity. Red points corresponds to detected steps.

In total, 99.53% of 1500 steps have been detected; 100% for test 1, test 2 and test 3, and 98% for test 4. The mean and standard deviation of stride-length (SL) estimates can be found in Figure 9 and Table5, respectively. Figure 9 represents the SL mean relative error with bars.

Calibrated MIMU22BL IMU shows the best results, with a mean relative error of 2.26%, followed by Xsens with %2.87. The worst results (5.04%) are obtained with the LSM6DS3 IMU. This error is increased by longer stride lengths (Tests 1-2 & 3-4), because of the accumulated error in data samples for longer times, without ZUPT correction. Also at higher speeds (Test 4) there is more error due to impact of the foot with the surface is greater and oscillations might be increased.

Figure 10 contains mean relative error of total travelled distance. In all cases, estimated distance is lower than actual distance (8 m). Mean errors are between -0.61% for Calibrated LSM6DS3 and 4.02% for LSM6DS3.

Moreover, we conducted the same tests with Xsens motion capture suit (MVN Animate), in order to analyse the efficacy of it. Results showed that error in estimations was higher than the achieved results of the single Xsens IMU in the foot, above 5% on stride length estimation error.

Errors are not only caused by the sensor or the processing algorithm, human errors should be take into account. Although there are visual references that determine where the foot should be placed, in practice, this can be difficult and errors of 1-2 cm can occur (they only account for 0.25% in total distance, but a significant 2.5% for SL). Having into account this, we are in the limit of our method with the tiled floor, so as to evaluate IMU errors, with Calibrated MIMU22BL below 2.5% in stride estimation error.

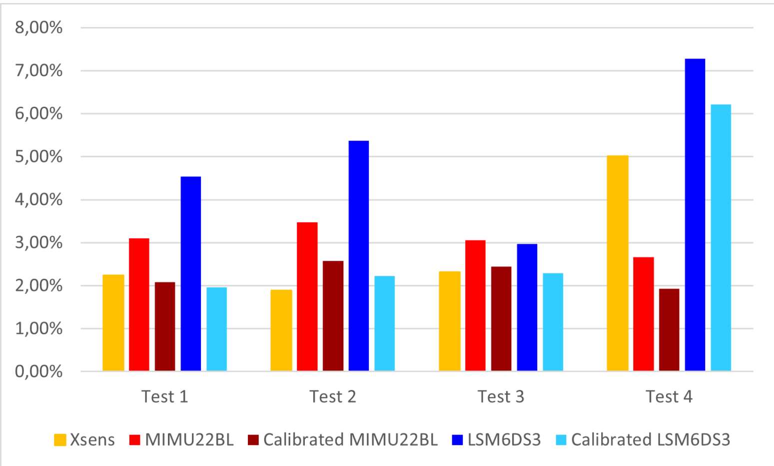

Figure 9: Stride Length Mean Relative Error. Yellow: Xsens, Red: MIMU22BL, Dark Red: Calibrated MIMU22BL, Blue: LSM6DS3 and Cyan: Calibrated LSM6DS3

We can clearly observe the effect of the calibration, with a benefit of 70% in the reduction of the SL estimation error, in MIMU22BL and LSM6DS3. During our investigations we observed that clock calibration for these sensors was the most important parameter in the reduction of SL errors.

In the AV tests in figures 1, 2, we can observe the improvement of new IMUs in the gyroscope noise with the Xsens, which is more than 10 years old. However accelerometer keeps being

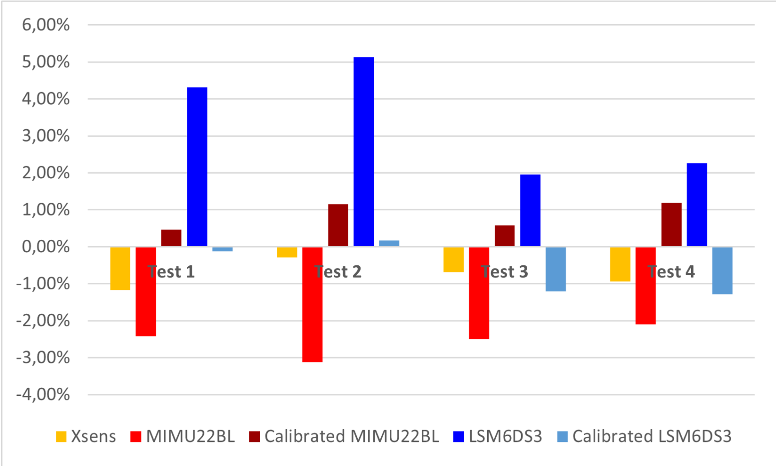

Figure 10: Total Distance Mean Relative Error. Yellow: Xsens, Red: MIMU22BL, Dark Red: Calibrated MIMU22BL, Blue: LSM6DS3 and Cyan: Calibrated LSM6DS3

Table 5
Stride Length Standard Deviation (meters)

IMU model	Test 1	Test 2	Test 3	Test 4	Mean
Xsens	0.019	0.029	0.022	0.111	0.045
MIMU22BL	0.021	0.038	0.022	0.032	0.028
Calibrated MIMU22BL	0.019	0.038	0.023	0.033	0.028
LSM6DS3	0.020	0.038	0.023	0.174	0.064
Calibrated LSM6DS3	0.018	0.035	0.022	0.170	0.061

better in Xsens. Comparing new IMUs, MIMU22BL outperforms LSM6DS3, with more bias stability and less noise in the accelerometer. Due to the fact that MIMU22BL has a fusion array of four IMUs. Calibrated MIMU22BL excel the rest of IMUs in stride length estimation, closely followed by Xsens. Xsens despite being much older, might have these great results due to factory calibration process which is much better than in the other low cost MEMS, and also adapts with temperature changes. In addition lower ranges in Xsens might help to track more accurately.

Taking into account these considerations, the effect of IMU noise is quite relevant, being Calibrated MIMU22BL the best sensor in AV and in SL estimation error and LSM6DS3 the worst sensor in both. But the tests carried out had only one total distance of 8 meters, so the influence of noise in long term is not noticeable in our study. We can assure that a refined algorithm for the step detection is crucial due to the effect in ZUPT correction it has. If a Step is not detected, the error will be accumulated in the stride length.

Analysing the differences in the sensors and its adjustment during the test, the weight and dimensions of PCB board that implemented the LSM6DS3 might have affected the results. Different placement of the IMU on the foot might have affected too.

After the basic calibration without external equipment's, explained in section 3, results show improvements in stride length estimation error. But Xsens still outperforms LSM6DS3.

6. Conclusion

In this paper we studied the influence of IMU noise on the accuracy of stride-length in gait analysis. Three IMUs were used, showing preliminary results when estimating stride lengths, with errors between 2.26% and 5.04% in different conditions of step length, velocity and five different subjects. Taking into account the SL errors found, the IMU's noise content (Random walk and bias instability) did have effect on our SL estimations. The use of the lowest sensing range is useful to reduce quantization noise, but increases the risk of clipping the IMU signal. Proper calibration is required to achieve better results, furthermore clock calibration has been the most important parameter in the improvements of the errors. On the other hand, we found that a robust algorithm to detect steps and stance intervals is very important when using ZUPT correction. The physical characteristics of the sensor and a secure attachment is also important to avoid sensor oscillations or displacements which may occur during gait. In the future, the authors will continue working on studying the noise influence in more extensive and exhaustive tests as well as, improving the step detection and stride length estimation algorithms.

7. Acknowledgments

Thanks to funding entities: the Spanish Ministry of Science, Grant Nos. MICROCEBUS RTI2018-095168-B-C55 (MCIU/AEI/FEDER, UE), REPNIN+ TEC2017-90808-REDT, the European Union NEXTPERCEPTION project Grant No. ECSEL-2019-2-RIA, Ref.: 876487, and G-STRIDE project (ref. M2451) Mapfre Ignacio Larramendi foundation.

References

[1] World Health Organization. https://www.who.int/ageing/about/facts/es/, March 2021.

[2] L. P. Fried et al., "Frailty in Older Adults: Evidence for a Phenotype," Journals Gerontol. Ser. A Biol. Sci. Med. Sci., vol. 56, no. 3, pp. M146–M157, 2001.

[3] F. Petraglia, L. Scarcella, G. Pedrazzi, L. Brancato, R. Puers, and C. Costantino, "Inertial sensors versus standard systems in gait analysis: A systematic review and meta-analysis," Eur. J. Phys. Rehabil. Med., vol. 55, no. 2, pp. 265–280, 2019.

[4] M. Patel, A. Pavic, and V. A. Goodwin, "Wearable inertial sensors to measure gait and posture characteristic differences in older adult fallers and non-fallers: A scoping review," Gait Posture, vol. 76, no. October 2019, pp. 110–121, 2020.

[5] L. Dasenbrock, A. Heinks, M. Schwenk, and J. M. Bauer, "Technology-based measurements for screening, monitoring and preventing frailty," Z. Gerontol. Geriatr., vol. 49, no. 7, pp. 581–595, 2016.

[6] M. Schwenk et al., "Frailty and technology: A systematic review of gait analysis in those with frailty," Gerontology, vol. 60, no. 1, pp. 79–89, 2013.

[7] R. Zhong and P. L. P. Rau, "Are cost-effective technologies feasible to measure gait in older adults? A systematic review of evidence-based literature," Archives of Gerontology and Geriatrics, vol. 87. 2020.

[8] J. Taborri, E. Palermo, S. Rossi, and P. Cappa, “Gait partitioning methods: A systematic review,” Sensors (Switzerland), vol. 16, no. 1, pp. 40–42, 2016.
[9] A. R. Jiménez, F. Seco, C. Prieto, and J. Guevara, “A comparison of pedestrian dead-reckoning algorithms using a low-cost MEMS IMU,” in WISP 2009 - 6th IEEE International Symposium on Intelligent Signal Processing - Proceedings, 2009, pp. 37–42.
[10] A. Peruzzi, U. Della Croce, and A. Cereatti, “Estimation of stride length in level walking using an inertial measurement unit attached to the foot: A validation of the zero velocity assumption during stance,” J. Biomech., vol. 44, no. 10, pp. 1991–1994, 2011.
[11] Wahlstrom, J., & Skog, I. (2021). Fifteen Years of Progress at Zero Velocity: A Review. IEEE Sensors Journal, 21(2). https://doi.org/10.1109/JSEN.2020.3018880
[12] T. Watanabe, T. Miyazawa, and J. Shibasaki, “A study on IMU-based stride length estimation for motor disabled subjects: A comparison under different calculation methods of rotation matrix,” in 2018 IEEE EMBS International Conference on Biomedical and Health Informatics, BHI 2018, 2018, vol. 2018–January, pp. 70–73.
[13] Wang, Y., Chernyshoff, A., & Shkel, A. M. (2020). Study on estimation errors in ZUPT-Aided pedestrian inertial navigation due to IMU noises. IEEE Transactions on Aerospace and Electronic Systems, 56(3), 2280–2291. https://doi.org/10.1109/TAES.2019.2946506.
[14] C. Mitschke, P. Kiesewetter, and T. L. Milani, “The effect of the accelerometer operating range on biomechanical parameters: Stride length, velocity, and peak tibial acceleration during running,” Sensors (Switzerland), vol. 18, no. 1, 2018.
[15] L. Zhou et al., “How we found our imu: Guidelines to IMU selection and a comparison of seven IMUs for pervasive healthcare applications,” Sensors (Switzerland), vol. 20, no. 15, pp. 1–28, 2020.
[16] C. Tunca, N. Pehlivan, N. Ak, B. Arnrich, G. Salur, and C. Ersoy, “Inertial sensor-based robust gait analysis in non-hospital settings for neurological disorders,” Sensors (Switzerland), vol. 17, no. 4, 2017.
[17] IEEE, “IEEE standard specification format guide and test procedure for single-axis interferometric fiber optic gyros,” IEEE Std 952-1997, 1998.
[18] N. El-Sheimy, H. Hou, and X. Niu, “Analysis and modeling of inertial sensors using allan variance,” IEEE Trans. Instrum. Meas., vol. 57, no. 1, pp. 140–149, 2008.
[19] M. Vagner, “MEMS Gyroscope Performance Comparison Using Allan Variance Method,” IEEE Instrum. Meas. Technol. Conf., vol. 2, no. 1, pp. 1–5, 2011.
[20] Oliver Woodman. Introduction to Inertial Navigation, January 2007.
[21] G. G.-V. Neira, Análisis del patrón de marcha mediante el diseño de un prototipo electrónico y una App de monitorización. End of degree project. URJC. 2020.
[22] Tedaldi, D., Pretto, A., & Menegatti, E. (2014). A robust and easy to implement method for IMU calibration without external equipments. Proceedings - IEEE International Conference on Robotics and Automation, 3042–3049. https://doi.org/10.1109/ICRA.2014.6907297
[23] Visi, F., Georgiou, T., Holland, S., Pinzone, O., Donaldson, G., & Tetley, J. (2017). Assessing the accuracy of an algorithm for the estimation of spatial gait parameters using inertial measurement units: Application to healthy subject and hemiparetic stroke survivor. ACM International Conference Proceeding Series, Part F1291. https://doi.org/10.1145/3077981.3078034